

Discovery of Isoindoline Amide Derivatives as Potent and Orally Bioavailable ADAMTS-4/5 Inhibitors for the Treatment of Osteoarthritis

Peng Zhao,^{*,§} Dong Liu,[§] Chunying Song,^{*} Di Li, Xinzhu Zhang, Ivana Horecny, Fengqi Zhang, Yuna Yan, Linghang Zhuang, Jing Li, Suxing Liu, Yuchang Mao, Jun Feng, Jian Liu, and Weikang Tao



Cite This: *ACS Pharmacol. Transl. Sci.* 2022, 5, 458–467



Read Online

ACCESS |



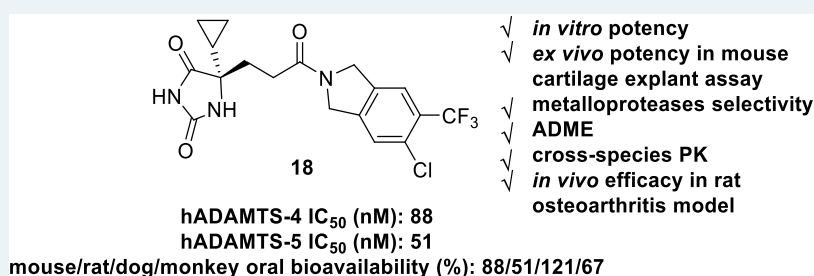
Metrics & More



Article Recommendations



Supporting Information



ABSTRACT: Osteoarthritis (OA) treatment is a highly unmet medical need. Development of a disease-modifying OA drug (DMOAD) is challenging with no approved drugs on the market. Inhibition of ADAMTS-4/5 is a promising OA therapeutics to target cartilage degradation and potentially can reduce joint pain and restore its normal function. Starting from the reported ADAMTS-5 inhibitor GLPG1972, we applied a scaffold hopping strategy to generate a novel isoindoline amide scaffold. Representative compound **18** showed high potency in ADAMTS-4/5 inhibition, as well as good selectivity over a panel of other metalloproteases. In addition, compound **18** exhibited excellent druglike properties and showed better pharmacokinetic (PK) profiles than GLPG1972 cross-species. Compound **18** demonstrated dose-dependent efficacy in two *in vivo* rat osteoarthritis models.

KEYWORDS: osteoarthritis, ADAMTS-4, ADAMTS-5, inhibitor, isoindoline, amide

Osteoarthritis (OA) is the most common chronic joint disease that affects the knee or hip with symptoms including joint pain and dysfunction.¹ OA occurs mostly in middle-aged and elderly people, and the global prevalence was about 654 million cases in 2020.² Pain and loss of functional capacity from OA are also accompanied by increased risks of additional diseases, such as diabetes, cancer, or cardiovascular disease.³ OA is a whole joint disease, the structural changes of which are found to be degradation of articular cartilage, synovitis, and alterations in subchondral bone and other periarticular tissues.⁴ Current osteoarthritis treatment methods are limited to drugs that only relieve symptoms such as pain or inflammation. No disease-modifying OA drug (DMOAD) has been approved, and the only option is joint replacement surgery for patients with severe degenerative joint disease. Thus, development of disease-modifying OA drugs to arrest or slow down disease progression is a highly unmet medical need.⁵ However, discovery and development of DMOAD are very challenging due to the complicated and not well-understood OA pathology, limited drug discovery efforts, a lack of *in vivo* efficacy models, and expensive and hard-to-design clinical trials to meet meaningful symptom improvement with concomitant structural benefits.

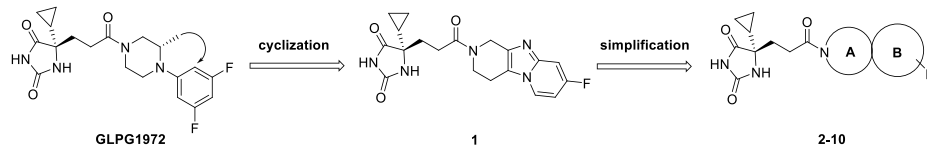
One major type of DMOAD is aimed at either reduction in cartilage degradation or stimulation of cartilage production. The principal function of cartilage in the joints is to provide the capability of load bearing and compression resistance to joints. The main component of cartilage is the extracellular matrix comprising aggrecan and collagen. Aggrecan interacts with hyaluronic acid in the synovial fluid to form aggregates that promote resistance to compression and deformation.⁶ Studies suggested that aggrecan plays a critical role in cartilage regulation. Aggrecan is a proteoglycan that possesses a core protein with covalently attached sulfated glycosaminoglycan (GAG) chains. Aggrecan can be cleaved by aggrecanases. Inhibition of aggrecanase activity can result in restoration of joint aggrecan levels, improvement in cartilage thickness, and reduction in bone hardening.⁷

Received: February 11, 2022

Published: June 22, 2022



Table 1. Discovery and Optimization of Bicyclic Amides 2–10



cmpd	Ring A-B	ADAMTS-4/5 IC ₅₀ (nM)	GSH adduct
GLPG1972		101/29	no
1		360/770	
2		2700/>10000	
3		>10000/>10000	
4		110/410	
5		42/37	yes
6		1700/6200	
7		5800/3600	
8		46/73	
9		15/37	
10		19/12	yes

ADAMTS (a disintegrin and metalloproteinase with thrombospondin motifs) is a family of zinc ion-dependent metalloproteinases. ADAMTS-4 (aggrecanase 1) and ADAMTS-5 (aggrecanase 2) are known to play primary roles in specific aggrecan degradation. ADAMTS-4 and ADAMTS-5 degrade aggrecan at Glu373–Ala374 in the interglobular domain and the regions with sulfated glycosaminoglycan chains.⁶ The level

of these cleaved GAGs can be measured to detect the activity of ADAMTS-4 and ADAMTS-5.

Several studies suggested that both ADAMTS-4 and ADAMTS-5 are important for human osteoarthritis disease.^{8–14} Therefore, inhibition of ADAMTS-5 and/or ADAMTS-4 to target cartilage breakdown has tremendous therapeutic potential in OA treatment. Several studies to develop ADAMTS-4/5 antibodies and small-molecule inhib-

itors have been reported. Merck KGaA developed a phase II-ready anti-ADAMTS-5 nanobody, M6495, and out-licensed it to Novartis in October 2020. A few scattered ADAMTS-4/5 small-molecule inhibitors from Wyeth,¹⁵ Japan Tobacco,¹⁶ GSK,¹⁷ AstraZeneca,¹⁸ Pfizer,¹⁹ DuPont,²⁰ Eli Lilly,^{21–23} and Galapagos^{24,25} were disclosed. AGG-523 and GLPG1972 entered phase I and phase II clinical trials, separately. GLPG1972 showed acceptable efficacy in *in vivo* rat OA models.²⁵ However, GLPG1972 did not meet its primary clinical endpoints in phase II clinical studies. Both GLPG1972 and ADAMTS-5 nanobody therapies were well tolerated and generally safe.^{26,27}

It is essential to distinguish the inhibition of ADAMTS-4/5 from other metzincin superfamily members, e.g., other ADAMTS family members, ADAMs (a disintegrin and metalloproteinases) and MMPs (matrix metalloproteinases). Nonselective MMP inhibitors resulted in several side effects, such as musculoskeletal syndrome (MSS), which hampered their clinical success in the treatment of OA disease.²¹ The active sites of MMPs have high structural homology to those of aggrecanases.²³ A well-tolerated ADAMTS-4/5 inhibitor for OA treatment should have a high level of selectivity over other MMPs and ADAMs.

Several cocrystal structures of small molecules with ADAMTS-4 and ADAMTS-5 were reported and provided basic guidance for rational drug design.^{19,21} Current small-molecule ADAMTS-4/5 inhibitors generally contain three sections: zinc-binding functionality (carboxylic acid, hydroxamic acid, reverse hydroxamate or hydantoin), a hydrophobic moiety, and a linker to put them together. It has been challenging to identify candidates composed of polar carboxylic acid and a highly lipophilic moiety to have moderate plasma protein binding and a good oral PK profile.^{15,16,24} Many hydroxamate drugs failed in development due to selectivity, toxicity, or stability issues.^{18–20} Hydantoin-based ADAMTS inhibitors showed promising potential with *in vitro* potency, PK properties, and *in vivo* efficacy.^{21–25} Eli Lilly developed a series of hydantoin-derived ADAMTS-4/5 inhibitors with excellent oral bioavailability. Another hydantoin molecule, GLPG1972 from Galapagos, finished phase II clinical trials.

Herein, we report the discovery and optimization of hydantoin-type ADAMTS-4/5 inhibitors featured by a novel isoindoline amide scaffold for the treatment of osteoarthritis. The most promising compound **18** showed high *in vitro* potency as an ADAMTS-4/5 inhibitor, good druglike properties, and oral bioavailability. Molecule **18** exhibited clear dose-dependent efficacy in two independent *in vivo* efficacy studies.

RESULTS AND DISCUSSION

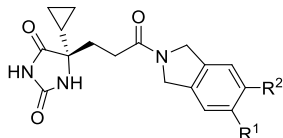
During our search for novel ADAMTS-5 inhibitors, we initially designed **1** as a potential inhibitor by intramolecular cyclization (Table 1). Human ADAMTS-4/5 inhibition testing showed that **1** has moderate potency, which prompted further optimization using different bicyclic amide scaffolds.

Although initial [6,5]-fused bicyclic compounds **2** and **3** totally lost ADAMTS-5 potency, gratifyingly, [5,6]-fused bicyclic compound **4** showed acceptable potency and [7,6]-fused bicycle **5** exhibited very decent inhibition activity to ADAMTS-4/5. Preliminary SAR exploration around [5,6]-fused bicycles revealed substitution on phenyl *ortho*-position (molecule **6**) was not tolerable. SAR from [7,6]-fused bicycles **5** also indicated that phenyl *ortho*-substitution (molecule **7**) led

to reduced potency. When the $-\text{OCH}_3$ group in **7** was moved from *ortho*- to *meta*-position, compound **8** had significantly improved ADAMTS-5 potency. Further modifications on *meta*-position by $-\text{F}$ and $-\text{CF}_3$ resulted in **9** and **10** with low double-digit nanomolar potency both in ADAMTS-4 and ADAMTS-5. However, [7,6]-fused bicycles **5** and **10** were found to be metabolic labile and tend to form glutathione (GSH) adduct by *in vitro* tests. As an effective tool to assess the likelihood of reactive metabolite formation, GSH adduct experiments allow the assessment of reactive metabolite-associated toxicity risks. To treat chronic diseases such as OA, safety profiling of DMOADs is one of the key parameters to the success of drug development. Thus, we focused on isoindoline-type [5,6]-fused bicycles to explore potent and safe ADAMTS-4/5 inhibitors without *in vitro* GSH adduct formation.

Monosubstitution on isoindoline *meta*-position suggested $-\text{CF}_3$ and $-\text{CHF}_2$ as the best groups in which $-\text{CF}_3$ was preferred based on synthetic feasibility (Table 2, molecules

Table 2. SAR of Isoindoline Amides 11–24



cmpd	R ¹	R ²	ADAMTS-4/5 IC ₅₀ (nM)	GSH adduct
11	H	F	310/370	
12	H	Cl	91/190	
13	H	CN	430/2000	
14	H	CF ₃	60/88	no
15	H	CHF ₂	30/66	
16	H	CH ₂ CF ₃	43/130	
17	F	CF ₃	110/62	
18	Cl	CF ₃	88/51	no
19	CHF ₂	CF ₃	1500/390	
20	CH ₃	CF ₃	23/27	yes
21	F	CHF ₂	56/100	
22	Cl	Cl	30/32	yes
23	CH ₃	Cl	43/130	
24	F	F	260/330	

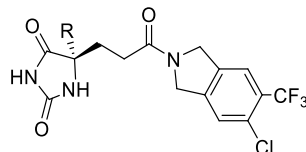
11–16). Furthermore, **14** with $-\text{CF}_3$ substitution did not form GSH adduct under our standard testing conditions. Based on **14**, additional substituents were installed on the adjacent position to make disubstituted compounds **17–20**. Compounds **18** and **20** both had improved ADAMTS-5 potency with retained or better ADAMTS-4 potency. Compounds **18** and **20** were subjected to GSH adduct tests, and GSH adduct was not observed for **18**. Interestingly, for compounds **14**, **17**, **18**, and **20**, all of which were bearing $-\text{CF}_3$ substitution, the apparent size of their second substituent group ($-\text{H} < -\text{F} < -\text{Cl} < -\text{CH}_3$) had the same order with ADAMTS-5 potency, 88 nM (**14**) < 62 nM (**17**) < 51 nM (**18**) < 17 nM (**20**). Other atom combinations in disubstituted derivatives **21–24** were also explored and **22** bearing di-Cl had the best potency. However, again, GSH adduct was found in **22** metabolite tests, which highlights the importance of the $-\text{CF}_3$ group with strong electron-withdrawing property to avoid GSH adduct formation (**18** vs **22**). Balanced by the potency and GSH adduct profile, **18** was selected for drug property evaluation and PK profiling. Computational modeling was also performed

Table 3. ADME and PK Profiling of 18^a

ADME	liver microsome $t_{1/2}$ (min) H/M/R	plasma (% unbound) H/M/R	PBS7.4 solubility (μM)	hERG IC_{50} (μM)	CYP IC_{50} (μM) (1A2, 2C9, 2C19, 2D6, 3A4-m, 3A4-t)
ADME	>139/>139/>67	6/6/3	37	>30	1.4/>30/>30/>30/>30/>30
PK	ig C_{max} (ng/mL)	iv $t_{1/2}$ (h)	iv CL (mL/min/kg)	ig AUC_{0-t} (ng/mL \times h)	F (%)
rat	1137	3.2	3.2	5283	51
mouse	1027	1.7	6.7	4285	88
dog	1374	6.1	2.6	14 729	121
monkey	714	7.3	2.7	7690	67
human (predicted)		7.4	1.9		82

^aSD rat and C57 mouse PK dose: iv 1 mpk, ig 2mpk. Beagle dog and cynomolgus monkey PK dose: iv 0.5 mpk, ig 2mpk.

Table 4. SAR of the Hydantoin Moiety in 18 and 25–27



cmpd	R	<i>in vitro</i> profiling		Rat PK (dose: iv 1 mpk, ig 2 mpk)				
		ADAMTS-4/5 IC_{50} (nM)	GSH adduct	ig C_{max} (ng/mL)	iv $t_{1/2}$ (h)	iv CL (mL/min/kg)	ig AUC_{0-t} (ng/mL \times h)	F (%)
18		88/51	no	1137	3.15	3.2	5283	51
25		54/25	no	7.1	1.13	68.6	5.6	4
26		74/32		271	1.29	8.8	891	24
27		100/39		131	0.57	20.4	218	12

to study the binding mode of fused bicyclic amides **10** and **18** (see Figure S1 and docking pose discussion).

Molecule **18** was very stable to human, mouse, and rat liver microsome metabolism with $t_{1/2}$ longer than 67 min (Table 3). Protein binding free fractions (%) of **18** in human, mouse, and rat plasma were 3–6%. Compound **18** had moderate PBS7.4 solubility and showed no appreciable inhibition on hERG ($\text{IC}_{50} > 30 \mu\text{M}$). Molecule **18** showed no appreciable inhibition on major CYP isoforms at 30 μM (our highest tested concentration), except moderate inhibition to CYP1A2, a minor CYP isoform, with an IC_{50} of 1.4 μM .

In rat PK analysis, compound **18** showed slow plasma clearance, good plasma $t_{1/2}$, a high plasma exposure level, and 51% oral bioavailability. In mouse, dog, and monkey PK studies, **18** demonstrated even better oral PK profiles with oral bioavailabilities of 88, 121, and 67%, respectively (Table 3). The excellent cross-species PK profiles of **18** suggested that it can potentially reach and maintain high exposure in both plasma and joint cartilage. Compound **18** was predicted to have slow clearance and high oral bioavailability of 82% in human PK (Table S1).

After the finding that CF_3 - and Cl-substituted isoindoline amide in **18** is the best right-side piece, SAR was shifted to the left-side hydantoin part. By replacing the cyclopropyl (cPr) moiety in **18** with aryl groups, molecules **25**–**27** were synthesized and evaluated (Table 4). All new compounds had improved *in vitro* ADAMTS-5 potency, among which **25** was the best. Compounds **25**–**27** were submitted for rat PK profiling. Unfortunately, none of them were able to show a PK profile as good as **18**, which suggested the importance of the hydantoin C5 –cPr group in the improvement of PK. The scientists from Galapagos also observed the same trend in their scaffold that the –cPr hydantoin analogues showed superior PK performance to aryl hydantoin counterparts.²⁴

Beyond ADAMTS-4 and ADAMTS-5, compounds **18**, **20**, **25**, **26**, and GLPG1972 were evaluated against a panel of proteases for selectivity (Table 5). These closely related, as well as various families of proteases, were selected based on their sequence and function similarity to ADAMTS-4/5, disease relevance, and commercial availability. Both **18** and **25** showed better selectivity among 12 other proteases than **20** and **26**. Also, **25** had a little bit better selectivity than **18**. Both compounds inhibited MMP2, MMP8, and MMP12 with

Table 5. Proteases Panel Selectivity of 18, 20, 25, 26, and GLPG1972

proteases	18 IC ₅₀ (nM)	20 IC ₅₀ (nM)	25 IC ₅₀ (nM)	26 IC ₅₀ (nM)	GLPG1972 IC ₅₀ (nM)
ADAMTS-4	88	23	54	74	101
ADAMTS-5	51	27	25	32	29
ADAM10	30 000	36 380	30 000	23 460	30 000
ADAM17	30 000	3817	30 000	2160	30 000
MMP1	30 000		30 000		30 000
MMP2	29		685		20
MMP3	2953		65 990		15 210
MMP7	30 000		30 000		30 000
MMP8	21	7	317	6.6	141
MMP9	23 620		30 000		14 800
MMP10	5345	257	30 000	401	30 000
MMP12	1.5		13		32
MMP13	6214	168	17 580	1476	13 190
MMP14	3611	174	16 180	270	4233

similar inhibition to that of GLPG1972, although slightly stronger MMP8 and MMP12 inhibition was observed in compound 18. Despite clean protease selectivity, molecule 25 was abandoned due to its extremely low plasma exposure with an oral bioavailability of 4% (Table 4).

Disease-related biology evaluation suggested no reported potential issues when inhibiting MMP2, MMP8, and MMP12. A recent selective MMP inhibitor survey suggested that MMP2, MMP9, and MMP13 are not involved in the musculoskeletal syndrome.²⁸ No toxicity phenotypes were reported from preclinical evaluations of MMP8 small-molecule inhibitors and nanobodies.^{29–31} MMP12 inhibitors AZD1236 and FP-025 were developed for the treatment of COPD (chronic obstructive pulmonary disease) and asthma. No serious adverse events were observed in their phase I clinical studies.^{32,33} GLPG1972 bears equipotent inhibition of ADAMTS-5, MMP2, and MMP12. GLPG1972 was well tolerated at all doses (up to 2100 mg once daily) in phase I clinical trials.²⁶ Thus, despite the slightly higher activity of 18 in inhibition of MMP2, MMP8, and MMP12 when compared to GLPG1972, the imperfect protease selectivity from inhibition of MMP12/8/2 does not raise safety and toxicity “red flags” on compound 18.

Molecule 18 was selected as the final candidate for efficacy studies after balancing potency, selectivity, safety profiling, ADME properties, and cross-species PK results. Inhibition of GAGs release in the mouse femoral head cartilage explant assay was explored to assess *ex vivo* potency of 18. According to the previous report, there was a good correlation between ADAMTS-5 inhibition and the mouse cartilage explant assay, but “a 100-fold shift was observed most likely reflecting easier

access of the compound to its soluble target in a biochemical assay than in a 3D matrix environment”.²⁴ In our case, molecule 18 reached a 50% inhibition of GAG release at 10 μ M concentration and the potency shift was about 200-fold (ADAMTS-5 biochemical IC₅₀ = 51 nM).

The next efficacy study was performed in a rat monoiodoacetate (MIA) model, a well-established preclinical model for osteoarthritis PD biomarker study.^{34–37} At day 0, MIA, an aerobic glycolysis inhibitor, was injected into the intra-articular space of the knee, which led to rapid progressive disruption of cartilage. Then, the rats were treated with compound 18 from day 3 to day 7. The levels of synovial ARGs (a proteolytic fragment of aggrecan) as the PD biomarker as well as PK parameters of 18 were measured to assess the efficacy.

When rats were treated with 25, 50, and 75 mpk of molecule 18 (BID dosing), the corresponding ARGs release inhibition was 18, 82, and 75%, respectively. Dose-dependent ARG inhibition and drug exposure level were observed for both 25 and 50 mpk. The exposure of 18 reached a plateau both in plasma and cartilage at 75 mpk. There was no significant efficacy difference between the 50 and 75 mpk groups (Table 6).

The last OA efficacy model used was the rat medial meniscus tear (MMT) model,^{38–40} in which we included one group of GLPG1972 as the control. In this model, cartilage damage and bone hardening were induced using surgical intervention by transection of the ligament and meniscus of the knee. Unilateral medial meniscal tear in rats resulted in rapidly progressive cartilage degenerative changes characterized by chondrocyte and proteoglycan loss, fibrillation, osteophyte formation, and chondrocyte cloning. Then, the rats were treated with 18 and GLPG1972 for 21 days. Endpoint efficacy evaluation in the joint included histopathologic examination to quantitatively assess cartilage damage and osteophyte formation.

The overall cartilage pathology was evaluated by the assessment of collagen matrix fibrillation or loss and chondrocyte death or loss. For quantitative measurements, the medial tibial plateau is divided into three zones to evaluate the pathology of different load-bearing areas. Molecule 18 reduced cartilage degeneration in both 25 and 50 mpk groups, and statistical significances were obtained in zone 2 and zone 3 (Figure 1). The total score of three zones for 18 at 50 mpk also had statistical significance. While GLPG1972 at 75 mpk also decreased cartilage degeneration scores compared to the vehicle control, the difference was not statistically significant.

The bone osteophyte score was generated by measuring the largest osteophyte in each section. Compound 18 at 50 mpk showed slightly better efficacy than GLPG1972 at 75 mpk,

Table 6. Compound 18 and GLPG1972 PK Results from Rat MIA PD Biomarker and Rat MMT Studies

cmpd	dose (po, mpk, BID)	rat MIA PD Biomarker		rat MMT		
		day 3 plasma AUC (h \times ng/mL) (n = 5) mean (95% CI)	day 7 cartilage concentration @ 3 h (ng/g) (n = 5) mean \pm SEM	day 1 plasma AUC (h \times ng/mL) (n = 4) mean (95% CI)	day 20 plasma AUC (h \times ng/mL) (n = 4) mean (95% CI)	day 21 cartilage AUC (h \times ng/g) (n = 3) mean (95% CI)
18	25	(50 507–77 431)	1973 \pm 346	(52 853–83 360)	(57 988–72 933)	(11 743–20 028)
18	50	(116 997–175 491)	4618 \pm 774	(100 018–205 838)	(165 234–205 017)	(20 987–69 494)
18	75	(112 578–207 374)	4177 \pm 1251			
GLPG1972	75			(16 852–25 966)	(18 260–26 477)	(3641–18 515)

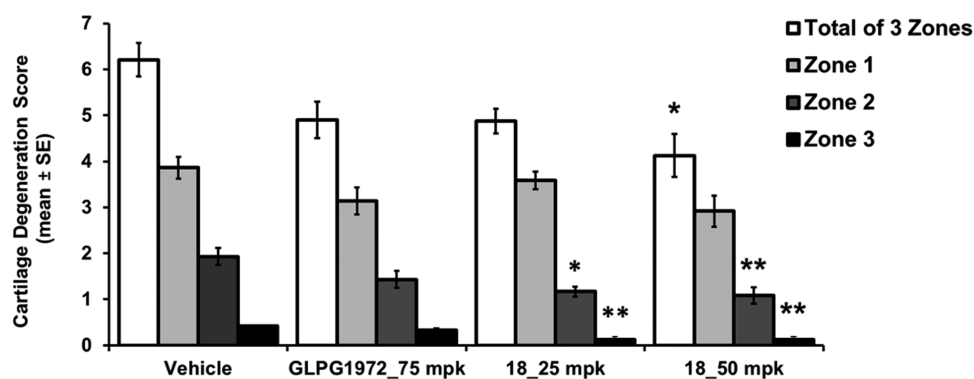


Figure 1. Compound 18 and GLPG1972 efficacy results in the rat MMT OA model: medial tibial cartilage degeneration score (* $p \leq 0.05$, ** $p \leq 0.01$, K–W test (Dunn's posthoc) vs vehicle).

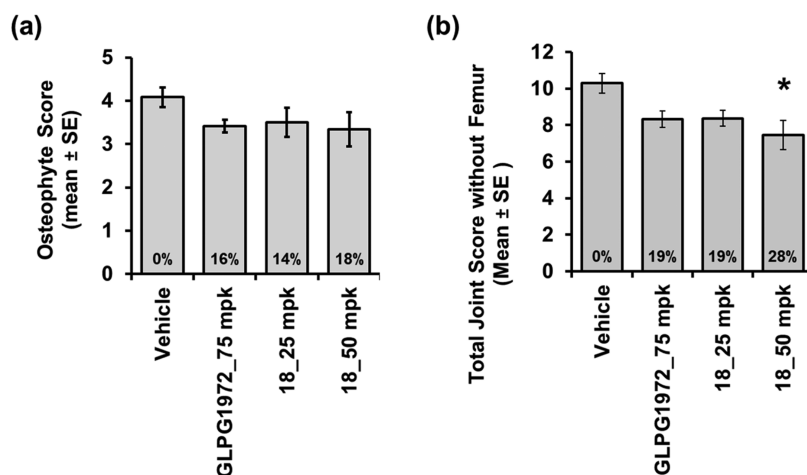


Figure 2. Compound 18 and GLPG1972 efficacy results in the rat MMT OA model: (a) medial tibial osteophyte score and (b) total joint score without a femur (* $p \leq 0.05$, K–W test (Dunn's posthoc) vs vehicle).

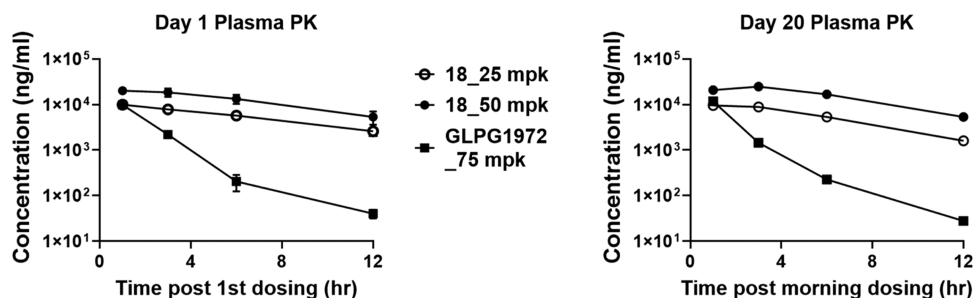


Figure 3. Compound 18 and GLPG1972 plasma PK curves in the rat MMT OA model.

although no statistical significance was achieved for all three groups (Figure 2a).

The cartilage degeneration and osteophyte scores were summed to determine the total joint score without a femur, which is the most important parameter in this MMT OA model. Compound 18 at 50 mpk significantly reduced the total joint score, while GLPG1972 at 75 mpk reduced the cartilage and bone damage scores to some extent, but it had no significant effect on the overall OA pathology (Figure 2b). It was reported that GLPG1972 reduced joint damage significantly in a female rat MNX model study.²⁵ Compared to its nonsignificant results from our male rat MMT model, this inconsistency might be related to the differences in the gender and sources of animals used in the two studies. The OA

diseases were induced by relatively complicated surgeries on rats performed by different surgeons. Any potential difference in disease extents induced could also contribute to the inconsistent results. Together, these results indicate that compound 18 has better efficacy than GLPG1972.

Plasma and cartilage PK results shown in Figure 3 and Table 6 clearly illustrated that 18 has better rat PK performance and target engagement than GLPG1972, which could be attributed to the longer $t_{1/2}$, steady plasma concentration, and higher plasma exposure of 18. Consistent with the results from the MIA PD biomarker study, dose-dependent plasma exposure of 18 was observed in the MMT study. No plasma drug accumulation happened in the period of this study from day 1 to day 20 (Table 6).

Concluded from the above efficacy studies, molecule **18** was able to inhibit mouse cartilage degradation in the *ex vivo* assay and demonstrated dose-dependent therapeutic efficacy in two *in vivo* preclinical rat OA models. Compound **18** showed inhibition of 82% of PD biomarker compared to the vehicle control in the MIA model. Compound **18** had a superior rat PK profile and biologically better total joint score in the surgery-induced rat MMT model than phase II clinical compound GLPG1972. Combined with excellent human PK prediction shown in Table 3, compound **18** would be expected to have better responses and therapeutic outcomes than GLPG1972 in human clinical testing.

GLPG1972 showed moderate clinical effects during OA treatment. Lessons learned from GLPG1972 clinical trials are “improving the bioavailability and specificity of drugs, and better selection of patients in clinical trials”.⁴¹ Compound **18** may display better clinical responses with its much better oral bioavailability than GLPG1972. However, its potency is not improved compared to GLPG1972, and its exposure plateaus when dosed high. These limitations remain as challenges when considering compound **18** for its further development into an efficacious oral small molecule for OA therapy. The risk of musculoskeletal syndrome (MSS) also needs to be investigated. MSS is considered “to be the result of nonselectivity (i.e., the inhibition of some other metalloproteases), or the combined inhibition of a combination of several critical MMPs”.⁴² Broad-spectrum MMP inhibitor batimastat and MMP1 sparing molecule PG-116800 both failed in clinical trials partially due to MSS.⁴² Although GLPG1972 has no reported MSS cases in the clinical trials and the inhibition of individual MMP2/8/12 does not raise toxicity “red flags,” molecule **18** has stronger inhibition of MMP8/12 than GLPG1972. The increased potential of MSS from combined strong inhibition of MMP8/12 and ADAMTS-4/5 is still open to be studied thoroughly.

CONCLUSIONS

We identified novel isoindoline amide **18** as a potent and orally bioavailable ADAMTS-4/5 inhibitor possessing MMP2/8/12 potency for the treatment of osteoarthritis. Compound **18** exhibited excellent cross-species PK and satisfactory ADME properties, especially clean *in vitro* liver safety as indicated by GSH adduct analysis. In the rat MIA PD biomarker study, compound **18** effectively inhibited aggrecan degradation as illustrated by an 82% ARG release inhibition. In the rat MMT osteoarthritis model, compound **18** significantly inhibited cartilage degeneration and improved joint damage score dose-dependently. The superior rat PK and biologically better *in vivo* rat efficacy of **18** over GLPG1972 prompted a new class of oral small-molecule drugs to be further investigated for the treatment of osteoarthritis.

METHODS

General chemistry and instrument information, compounds' synthetic procedure, molecular modeling, and ADME and PK studies are described in the Supporting Information.

The animal experimental protocol used in this study was approved by the Institutional Animal Care and Use Committees (IACUC) of Bolder BioPATH. The experiments were conducted in accordance with the Guiding Principles for the Care and Use of Laboratory Animals and complied with the ARRIVE guidelines. All animals survived to study

termination, and no statistical differences in absolute body weight gain were observed between test groups and vehicle groups. Vehicle: (5% dimethyl sulfoxide [DMSO], 20% PEG400, 70% (10% D- α -tocopheryl poly(ethylene glycol) 1000 succinate [TPGS]), and 5% (1% hydroxypropyl methylcellulose [HPMC])).

In Vitro Fluorescence Assay of ADAMTS-4 or ADAMTS-5 Activity. A FRET (fluorescence resonance energy transfer) peptide was cleaved by recombinant ADAMTS-4 or ADAMTS-5 proteins into two separate fragments, resulting in an increase of the fluorescence signal that was quantified. The peptide was 5-FAM-TEGEARGSVILLK(S-TAMRA)K-NH₂, custom-synthesized from ANASPEC. ADAMTS-4 recombinant protein (catalog# 4307-AD) and ADAMTS-5 recombinant protein (catalog# 2198-AD) were purchased from R&D Systems.

An assay buffer containing 50 mM HEPES pH 7.5, 100 mM NaCl, 5 mM CaCl₂, 0.1% CHAPS, and 5% glycerol was prepared. A volume of 2.5 μ L of the compound in the assay buffer was dispensed to a 384-well plate, and 2.5 μ L of ADAMTS-4 or ADAMTS-5 protein (final concentration in the reaction was 10 nM) was added. The compounds and proteins were preincubated at room temperature for 15 min. Then, 5 μ L of the substrate was added to each well. The final substrate concentrations for ADAMTS-4 and ADAMTS-5 were 15 and 8 μ M, respectively. The fluorescence signal in each well was determined after incubation at 37 °C for 3 h on a TECAN plate reader (excitation, 490 nm; emission, 520 nm).

The data was inputted into GraphPad Prism, and the IC₅₀ values were calculated using function “log (inhibitor) vs response – variable slope (four parameters)”.

Protease Selectivity. Protease panel selectivity was performed by Reaction Biology (1 Great Valley Pkwy #18, Malvern, PA).

Mouse Femoral Head Cartilage Explant Assay. Fresh mouse femoral head cartilage was treated with IL-1 α protein (Sigma-Aldrich, catalog# I2778) in culture media to induce cartilage catabolism. Then, the GAGs attached to the cleaved aggrecan fragments (released into the media) and the GAGs attached to the intact aggrecan were measured by dimethylmethylene blue dye in the Glycosaminoglycans Assay Kit (Chondrex, catalog# 6022).

Femoral head cartilage samples were isolated from mice (25 days old, male, C57BL/6, from Charles River Lab) and put into 2.0 mL tubes filled up with media (DMEM, 10% FBS, 4 mM glutamine, penicillin–streptomycin, 20 mM HEPES). About 200 μ L of media without FBS was added to each well of a 48-well plate, and one piece of cartilage was transferred to a well in the plate. Then, the media was aspirated, and compounds and IL-1 α protein were added to the plate in a total volume of 400 μ L of fresh media without FBS. The final concentration of IL-1 α was 1 ng/mL. The plate was incubated at 37 °C for 72 h in a humidified incubator with a 5% CO₂ supply.

The supernatant was transferred to a 1.5 mL tube and kept at –20 °C. Each cartilage sample was transferred to another 1.5 mL tube containing 400 μ L of freshly made papain solution. The papain solution contained 125 μ g/mL papain (Sigma-Aldrich, catalog# P3125), 0.1 M sodium acetate (Sigma-Aldrich, catalog# S7899), pH 5.5, 5 mM EDTA, and 5 mM L-cysteine–HCl (Sigma-Aldrich, catalog# C7880). The cartilage samples were kept rocking in a 60 °C water bath for 24 h.

The lysates were vortexed for 10 s and spun at 10 000 rpm for 2 min. Both the supernatant and the lysate samples were diluted with PBS and mixed with 100 μ L of dye from the Glycosaminoglycans Assay Kit. The optical density from each well was determined with a TECAN plate reader set to a wavelength of 525 nm.

The concentrations of GAGs in the supernatant and lysates were determined based on the standard curve with a dose range of chondroitin sulfate provided in the kit. The percentage of GAG release was calculated as follows

$$\text{GAG\%} = \left(\frac{[\text{GAG}]_{\text{supernatant}}}{[\text{GAG}]_{\text{supernatant}} + [\text{GAG}]_{\text{lysate}}} \right) \times 100\%$$

The test compound effect was expressed as the percent of inhibition using the following formula

$$\text{inhibition\%} = \left(\frac{1h \text{ GAG\%}(\text{compound} + \text{IL1}\alpha) - \text{GAG\%}(\text{vehicle})}{\text{GAG\%}(\text{vehicle} + \text{IL1c}) - \text{GAG\%}(\text{vehicle})} \right) \times 100\%$$

Rat MIA PD Biomarker Experiment. Male Lewis rats were randomized by body weight into groups ($n = 5$) on study day 0. After randomization, the animals were anesthetized with isoflurane (VetOne, catalog# 502017), and the right knees were given a single (2 mg) intra-articular (IA) injection of sodium iodoacetate (MIA) (40 μ L of 50 mg/mL, Sigma, catalog# 12512-25G) in saline (VetOne, catalog# 1510224). The contralateral left knee was injected IA with saline. The rats were dosed twice daily (BID) with 18 (25, 50, and 75 mg/kg) by the oral (PO) route from day 3 to day 7.

Body weight measurements were performed on study days 0, 3, and 7. Interim blood collection for plasma occurred 1, 3, and 12 h postdose on day 3 and 1 h following the morning dose on study day 7. The animals were euthanized for terminal sample collection 3 h following the morning dose on day 7. Whole blood was processed for plasma (K3EDTA, 2 \times 1 mL/rat), which was stored frozen at -80 $^{\circ}$ C. Right and left knees were lavaged twice by injecting 100 μ L of EDTA saline into the joint followed by repeated flexion and extension. The fluid was removed, placed on wet ice, and centrifuged within 10 min of collection. The resulting supernatant was poured into tubes on dry ice and stored frozen at -80 $^{\circ}$ C. Shavings of articular cartilage from the tibial plateau of left knees were collected into 1.5 mL Eppendorf tubes and flash-frozen in liquid nitrogen.

ARG levels in synovial fluid were measured using ELISA. BC-3 antibody (antiaggrecan ARGxx antibody [BC-3], Abcam, catalog# ab3773) was purified and conjugated to horseradish peroxidase (HRP). ELISA plates (NUNC# 473709) were coated with aggrecan antibody (ThermoFisher# AHP0022) at 10 μ g/mL, 100 μ L/well, at 4 $^{\circ}$ C overnight. The plates were washed with PBST (PBS + 0.05% Tween) three times and blocked in buffer (2% BSA in PBST) shaking at room temperature for 90 min. The samples were washed three times; synovial fluid (100 μ L samples) was added and incubated at room temperature for 2 h. The samples were washed three times, and 100 μ L of BC-3 antibody conjugated to HRP was added at room temperature for 90 min. Samples were washed again, and then 100 μ L of 3,3',5,5'-tetramethylbenzidine (TMB) was added at room temperature for 15 min. The stop solution (0.25 M sulfuric acid) was added, and the results were detected at OD450-OD620. Results were normalized using urea.

Rat MMT Efficacy Study. Male Lewis rats were randomized by body weight into groups ($n = 12$) on study day -1 . On study day 0, the animals underwent surgery to perform a unilateral medial meniscal tear on the right knee. The animals were treated with PO twice daily (BID) with 18 (25 and 50 mg/kg) and GLPG1972 (75 mg/kg) or vehicle. The rats were dosed on days 0–20 (animals 1, 5, and 9 per group) or days 0–21 (all other animals) and were euthanized for necropsy on day 21 postsurgery (1, 3, 6, or 12 h after the final dose). Endpoints for evaluation of therapeutic efficacy included histopathologic examination to quantitatively assess cartilage damage and osteophyte formation. Assessment is made based on guidelines from the Osteoarthritis Research Society International (OARSI).

■ ASSOCIATED CONTENT

Supporting Information

The Supporting Information is available free of charge at <https://pubs.acs.org/doi/10.1021/acspsci.2c00023>.

Human PK prediction of compound 18, molecular modeling and pose discussion, general chemistry information, synthetic procedures for compounds 1–27, ADME and PK information, references, and NMR spectra of all new compounds (PDF)

■ AUTHOR INFORMATION

Corresponding Authors

Peng Zhao – Eternity Bioscience Inc., Cranbury, New Jersey 08512, United States; orcid.org/0000-0003-1536-9575; Email: pengebi.zhao@hengrui.com

Chunying Song – Eternity Bioscience Inc., Cranbury, New Jersey 08512, United States; Email: song_cy@hotmail.com

Authors

Dong Liu – Eternity Bioscience Inc., Cranbury, New Jersey 08512, United States

Di Li – Eternity Bioscience Inc., Cranbury, New Jersey 08512, United States

Xinzhu Zhang – Eternity Bioscience Inc., Cranbury, New Jersey 08512, United States

Ivana Horecny – Eternity Bioscience Inc., Cranbury, New Jersey 08512, United States

Fengqi Zhang – Eternity Bioscience Inc., Cranbury, New Jersey 08512, United States

Yuna Yan – Shanghai Hengrui Pharmaceutical Co. Ltd., Shanghai 200245, China

Linghang Zhuang – Eternity Bioscience Inc., Cranbury, New Jersey 08512, United States

Jing Li – Eternity Bioscience Inc., Cranbury, New Jersey 08512, United States

Suxing Liu – Eternity Bioscience Inc., Cranbury, New Jersey 08512, United States

Yuchang Mao – Shanghai Hengrui Pharmaceutical Co. Ltd., Shanghai 200245, China

Jun Feng – Shanghai Hengrui Pharmaceutical Co. Ltd., Shanghai 200245, China

Jian Liu – Eternity Bioscience Inc., Cranbury, New Jersey 08512, United States; orcid.org/0000-0002-8408-7689

Weikang Tao – Shanghai Hengrui Pharmaceutical Co. Ltd., Shanghai 200245, China

Complete contact information is available at: <https://pubs.acs.org/doi/10.1021/acspsci.2c00023>

Author Contributions

[§]P.Z. and D. Liu contributed equally to this work and share the first authorship. P.Z., D. Liu, and C.S. designed the experiments; D. Li and I.H. performed biochemical assays and *ex vivo* mouse cartilage explant assays; X.Z., F.Z., and P.Z. synthesized the compounds; Y.Y. conducted molecular modeling; C.S. and S.L. coordinated *in vivo* efficacy studies with CROs and conducted data analyses; Y.M. contributed to PK studies and prediction; P.Z., D. Liu, C.S., J.L., S.L., L.Z., F.J., J.L., and W.T. interpreted experiment results; P.Z. and C.S. wrote the manuscript with contribution from D. Liu, J.L., S.L., L.Z., F.J., J.L., and W.T. All authors contributed to data analysis and reviewed the manuscript.

Notes

The authors declare the following competing financial interest(s): All authors were employees of Eternity Bioscience Inc. or Shanghai Hengrui Pharmaceutical Co. at the time this work was performed and may hold shares or share options in the company.

ACKNOWLEDGMENTS

This work was supported by Eternity Bioscience Inc. and Shanghai Hengrui Pharmaceutical Co. Ltd., subsidiaries of Jiangsu Hengrui Medicine. The authors acknowledge the help and great discussions in rat MIA PD biomarker and rat MMT efficacy studies by Dr. Alison M. Bendele, and Jacob Favret from Bolder BioPATH. The authors thank the manuscript preparation support and discussion from Dr. Chang Bai, Dr. Feng He, Dr. Hong Wan, Dr. Hilary Wilkinson, Dr. Lin Yan, and Dr. Xun Li. Part of the compound synthesis was performed at Medicilon. Initial ADAMTS protein expression and purification by Dr. Tongyuan Li and metabolite identification from Dr. Chunyong He are appreciated. The authors are thankful to project coordination and management from Hongli Chen.

ABBREVIATIONS

OAosteoarthritis; DMOADdisease-modifying OA drug; ADAMTSdisintegrin and metalloproteinase with thrombospondin motifs; ADAMdisintegrin and metalloproteinases; MMPmatrix metalloproteinase; MSSmusculoskeletal syndrome; GAGglycosaminoglycan; MIAmonoiodoacetate; MMTmedial meniscus tear; ARGproteolytic fragment of aggrecan; COPDchronic obstructive pulmonary disease; PDpharmacodynamics; SARstructure–activity relationship; ADMEabsorption, distribution, metabolism, and excretion; GSHglutathione; CYPcytochrome P450; CYP 3A4–mCYP 3A4 probed with midazolam; CYP 3A4–tCYP 3A4 probed with testosterone; Hhuman; Mmice; Rrat; PBS7.4phosphate-buffered saline solution of pH 7.4; hERGhuman ether-à-go-go-related gene; PKpharmacokinetics; AUCthe area under the curve; mpkmg/kg; $T_{1/2}$ half-life of the compound exposure in plasma; CLclearance; C_{max} maximum concentration of the compound in plasma; Foral bioavailability; N/Anot available; ivintravenous; igintragastrical; POper os, from the Latin for “by mouth”; BIDbis in die, from the Latin for “twice a day”; SEMstandard error of mean

REFERENCES

- (1) Rezuş, E.; Burlui, A.; Cardoneanu, A.; Macovei, L. A.; Tamba, B. I.; Rezuş, C. From pathogenesis to therapy in knee osteoarthritis: bench-to-bedside. *Int. J. Mol. Sci.* **2021**, *22*, 2697.
- (2) Cui, A.; Li, H.; Wang, D.; Zhong, J.; Chen, Y.; Lu, H. Global, regional prevalence, incidence and risk factors of knee osteoarthritis in population-based studies. *EClinicalMedicine* **2020**, *29–30*, No. 100587.
- (3) Valdes, A. M.; Stocks, J. Osteoarthritis and ageing. *Eur. Med. J.* **2018**, *3*, 116–123.
- (4) Goldring, M. B.; Otero, M. Inflammation in osteoarthritis. *Curr. Opin. Rheumatol.* **2011**, *23*, 471–478.
- (5) Oo, W. M.; Little, C.; Duong, V.; Hunter, D. J. The development of disease-modifying therapies for osteoarthritis (DMOADs): The evidence to date. *Drug Des. Dev. Ther.* **2021**, *15*, 2921–2945.
- (6) Verma, P.; Dalal, K. ADAMTS-4 and ADAMTS-5: key enzymes in osteoarthritis. *J. Cell. Biochem.* **2011**, *112*, 3507–3514.
- (7) Pratta, M. A.; Yao, W.; Decicco, C.; Tortorella, M. D.; Liu, R. Q.; Copeland, R. A.; Magolda, R.; Newton, R. C.; Trzaskos, J. M.; Arner, E. C. Aggrecan protects cartilage collagen from proteolytic cleavage. *J. Biol. Chem.* **2003**, *278*, 45539–45545.
- (8) Glasson, S. S.; Askew, R.; Sheppard, B.; Carito, B. A.; Blanchet, T.; Ma, H. L.; Flannery, C. R.; Kanki, K.; Wang, E.; Peluso, D.; Yang, Z.; Majumdar, M. K.; Morris, E. A. Characterization of and osteoarthritis susceptibility in ADAMTS-4-knockout mice. *Arthritis Rheum.* **2004**, *50*, 2547–2558.
- (9) Glasson, S. S.; Askew, R.; Sheppard, B.; Carito, B.; Blanchet, T.; Ma, H. L.; Flannery, C. R.; Peluso, D.; Kanki, K.; Yang, Z.; Majumdar, M. K.; Morris, E. A. Deletion of active ADAMTS5 prevents cartilage degradation in a murine model of osteoarthritis. *Nature* **2005**, *434*, 644–648.
- (10) Stanton, H.; Rogerson, F. M.; East, C. J.; Golub, S. B.; Lawlor, K. E.; Meeker, C. T.; Little, C. B.; Last, K.; Farmer, P. J.; Campbell, I. K.; Fourie, A. M.; Fosang, A. J. ADAMTS5 is the major aggrecanase in mouse cartilage *in vivo* and *in vitro*. *Nature* **2005**, *434*, 648–652.
- (11) Song, R. H.; Tortorella, M. D.; Malfait, A. M.; Alston, J. T.; Yang, Z.; Arner, E. C.; Griggs, D. W. Aggrecan degradation in human articular cartilage explants is mediated by both ADAMTS-4 and ADAMTS-5. *Arthritis Rheum.* **2007**, *56*, 575–585.
- (12) Roach, H. I.; Yamada, N.; Cheung, K. S.; Tilley, S.; Clarke, N. M.; Oreffo, R. O.; Kokubun, S.; Bronner, F. Association between the abnormal expression of matrix-degrading enzymes by human osteoarthritic chondrocytes and demethylation of specific CpG sites in the promoter regions. *Arthritis Rheum.* **2005**, *52*, 3110–3124.
- (13) Malfait, A. M.; Liu, R. Q.; Ijiri, K.; Komiya, S.; Tortorella, M. D. Inhibition of ADAM-TS4 and ADAM-TS5 prevents aggrecan degradation in osteoarthritic cartilage. *J. Biol. Chem.* **2002**, *277*, 22201–22208.
- (14) Naito, S.; Shiomi, T.; Okada, A.; Kimura, T.; Chijiwa, M.; Fujita, Y.; Yatabe, T.; Komiya, K.; Enomoto, H.; Fujikawa, K.; Okada, Y. Expression of ADAMTS4 (aggrecanase-1) in human osteoarthritic cartilage. *Pathol. Int.* **2007**, *57*, 703–711.
- (15) Chockalingam, P. S.; Sun, W.; Rivera-Bermudez, M. A.; Zeng, W.; Dufield, D. R.; Larsson, S.; Lohmander, L. S.; Flannery, C. R.; Glasson, S. S.; Georgiadis, K. E.; Morris, E. A. Elevated aggrecanase activity in a rat model of joint injury is attenuated by an aggrecanase specific inhibitor. *Osteoarthritis Cartilage* **2011**, *19*, 315–323.
- (16) Shiozaki, M.; Maeda, K.; Miura, T.; Kotoku, M.; Yamasaki, T.; Matsuda, I.; Aoki, K.; Yasue, K.; Imai, H.; Ubukata, M.; Suma, A.; Yokota, M.; Hotta, T.; Tanaka, M.; Hase, Y.; Haas, J.; Fryer, A. M.; Laird, E. R.; Littmann, N. M.; Andrews, S. W.; Josey, J. A.; Mimura, T.; Shinozaki, Y.; Yoshiuchi, H.; Inaba, T. Discovery of (1S,2R,3R)-2,3-dimethyl-2-phenyl-1-sulfamidocyclopropanecarboxylates: novel and highly selective aggrecanase inhibitors. *J. Med. Chem.* **2011**, *54*, 2839–2863.
- (17) Deng, H.; O’Keefe, H.; Davie, C. P.; Lind, K. E.; Acharya, R. A.; Franklin, G. J.; Larkin, J.; Matico, R.; Neeb, M.; Thompson, M. M.; Lohr, T.; Gross, J. W.; Centrella, P. A.; O’Donovan, G. K.; Bedard, K. L.; van Vloten, K.; Mataruse, S.; Skinner, S. R.; Belyanskaya, S. L.; Carpenter, T. Y.; Shearer, T. W.; Clark, M. A.; Cuozzo, J. W.; Arico-Muendel, C. C.; Morgan, B. A. Discovery of highly potent and selective small molecule ADAMTS-5 inhibitors that inhibit human

cartilage degradation via encoded library technology (ELT). *J. Med. Chem.* **2012**, *55*, 7061–7079.

(18) De Savi, C.; Pape, A.; Cumming, J. G.; Ting, A.; Smith, P. D.; Burrows, J. N.; Mills, M.; Davies, C.; Lamont, S.; Milne, D.; Cook, C.; Moore, P.; Sawyer, Y.; Gerhardt, S. The design and synthesis of novel N-hydroxyformamide inhibitors of ADAM-TS4 for the treatment of osteoarthritis. *Bioorg. Med. Chem. Lett.* **2011**, *21*, 1376–1381.

(19) Shieh, H. S.; Mathis, K. J.; Williams, J. M.; Hills, R. L.; Wiese, J. F.; Benson, T. E.; Kiefer, J. R.; Marino, M. H.; Carroll, J. N.; Leone, J. W.; Malfait, A. M.; Arner, E. C.; Tortorella, M. D.; Tomasselli, A. High resolution crystal structure of the catalytic domain of ADAMTS-5 (aggrecanase-2). *J. Biol. Chem.* **2008**, *283*, 1501–1507.

(20) Yao, W.; Wasserman, Z. R.; Chao, M.; Reddy, G.; Shi, E.; Liu, R. Q.; Covington, M. B.; Arner, E. C.; Pratta, M. A.; Tortorella, M.; Magolda, R. L.; Newton, R.; Qian, M.; Ribadeneira, M. D.; Christ, D.; Wexler, R. R.; Decicco, C. P. Design and synthesis of a series of (2R)-N(4)-hydroxy-2-(3-hydroxybenzyl)-N(1)-[(1S,2R)-2-hydroxy-2,3-dihydro-1H-inden-1-yl]butanediamide derivatives as potent, selective, and orally bioavailable aggrecanase inhibitors. *J. Med. Chem.* **2001**, *44*, 3347–3350.

(21) Durham, T. B.; Klimkowski, V. J.; Rito, C. J.; Marimuthu, J.; Toth, J. L.; Liu, C.; Durbin, J. D.; Stout, S. L.; Adams, L.; Swearingen, C.; Lin, C.; Chambers, M. G.; Thirunavukkarasu, K.; Wiley, M. R. Identification of potent and selective hydantoin inhibitors of aggrecanase-1 and aggrecanase-2 that are efficacious in both chemical and surgical models of osteoarthritis. *J. Med. Chem.* **2014**, *57*, 10476–10485.

(22) Wiley, M. R.; Durham, T. B.; Adams, L. A.; Chambers, M. G.; Lin, C.; Liu, C.; Marimuthu, J.; Mitchell, P. G.; Mudra, D. R.; Swearingen, C. A.; Toth, J. L.; Weller, J. M.; Thirunavukkarasu, K. Use of osmotic pumps to establish the pharmacokinetic-pharmacodynamic relationship and define desirable human performance characteristics for aggrecanase inhibitors. *J. Med. Chem.* **2016**, *59*, 5810–5822.

(23) Durham, T. B.; Marimuthu, J.; Toth, J. L.; Liu, C.; Adams, L.; Mudra, D. R.; Swearingen, C.; Lin, C.; Chambers, M. G.; Thirunavukkarasu, K.; Wiley, M. R. A highly selective hydantoin inhibitor of aggrecanase-1 and aggrecanase-2 with a low projected human dose. *J. Med. Chem.* **2017**, *60*, 5933–5939.

(24) Brebion, F.; Gosmini, R.; Deprez, P.; Varin, M.; Peixoto, C.; Alvey, L.; Jary, H.; Bienvenu, N.; Triballeau, N.; Blanque, R.; Cottreaux, C.; Christophe, T.; Vandervoort, N.; Mollat, P.; Touitou, R.; Leonard, P.; De Ceuninck, F.; Botez, I.; Monjardet, A.; van der Aar, E.; Amantini, D. Discovery of GLPG1972/S201086, a potent, selective, and orally bioavailable ADAMTS-5 inhibitor for the treatment of osteoarthritis. *J. Med. Chem.* **2021**, *64*, 2937–2952.

(25) Clement-Lacroix, P.; Little, C. B.; Smith, M. M.; Cottreaux, C.; Merciris, D.; Meurisse, S.; Mollat, P.; Touitou, R.; Brebion, F.; Gosmini, R.; De Ceuninck, F.; Botez, I.; Lepescheux, L.; van der Aar, E.; Christophe, T.; Vandervoort, N.; Blanqué, R.; Comas, D.; Deprez, P.; Amantini, D. Pharmacological characterization of GLPG1972/S201086, a potent and selective small-molecule inhibitor of ADAMTS-5. *Osteoarthritis Cartilage* **2022**, *30*, 291–301.

(26) Aar, E.; Deckx, H.; Dupont, S.; Fieuw, A.; Delage, S.; Larsson, S.; Struglics, A.; Lohmander, S. L.; Lalande, A.; Leroux, E.; Amantini, D.; Passier, P. Safety, pharmacokinetics, and pharmacodynamics of the ADAMTS-5 inhibitor GLPG1972/S201086 in healthy volunteers and participants with osteoarthritis of the knee or hip. *Clin. Pharmacol. Drug Dev.* **2022**, *11*, 112–122.

(27) Guehring, H.; Balchen, T.; Goteti, K.; Sonne, J.; Ladel, C.; Ona, V.; Moreau, F.; Bay-Jensen, A.; Bihlet, A. R. Safety, tolerability, pharmacokinetics and pharmacodynamics of single ascending doses of the anti-ADAMTS-5 nanobody, M6495, in healthy male subjects: A phase I, placebo-controlled, first-in-human study. *Arthritis Rheumatol.* **2019**, *71*, 10.

(28) Fields, G. B. The rebirth of matrix metalloproteinase inhibitors: moving beyond the dogma. *Cells* **2019**, *8*, 984.

(29) Folgueras, A. R.; Fueyo, A.; García-Suárez, O.; Cox, J.; Astudillo, A.; Tortorella, P.; Campestre, C.; Gutiérrez-Fernández, A.;

Fanjul-Fernández, M.; Pennington, C. J.; Edwards, D. R.; Overall, C. M.; López-Otín, C. Collagenase-2 deficiency or inhibition impairs experimental autoimmune encephalomyelitis in mice. *J. Biol. Chem.* **2008**, *283*, 9465–9474.

(30) Albaiceta, G. M.; Gutierrez-Fernández, A.; García-Prieto, E.; Puente, X. S.; Parra, D.; Astudillo, A.; Campestre, C.; Cabrera, S.; Gonzalez-Lopez, A.; Fueyo, A.; Taboada, F.; López-Otín, C. Absence or inhibition of matrix metalloproteinase-8 decreases ventilator-induced lung injury. *Am. J. Respir. Cell Mol. Biol.* **2010**, *43*, 555–563.

(31) Demeestere, D.; Dejonckheere, E.; Steeland, S.; Hulpiau, P.; Haustraete, J.; Devoogdt, N.; Wichert, R.; Becker-Pauly, C.; Van Wonerghem, E.; Dewaele, S.; Van Imschoot, G.; Aerts, J.; Arckens, L.; Saey, Y.; Libert, C.; Vandenbroucke, R. E. Development and validation of a small single-domain antibody that effectively inhibits matrix metalloproteinase 8. *Mol. Ther.* **2016**, *24*, 890–902.

(32) Magnussen, H.; Watz, H.; Kirsten, A.; Wang, M.; Wray, H.; Samuelsson, V.; Mo, J.; Kay, R. Safety and tolerability of an oral MMP-9 and -12 inhibitor, AZD1236, in patients with moderate-to-severe COPD: a randomised controlled 6-week trial. *Pulm. Pharmacol. Ther.* **2011**, *24*, 563–570.

(33) Abd-Elaziz, K.; Voors-Pette, C.; Wang, K. L.; Pan, S.; Lee, Y.; Mao, J.; Li, Y.; Chien, B.; Lau, D.; Diamant, Z. First-in-Man safety, tolerability, and pharmacokinetics of a novel and highly selective inhibitor of matrix metalloproteinase-12, FP-025: results from two randomized studies in healthy subjects. *Clin. Drug Invest.* **2021**, *41*, 65–76.

(34) Chandran, P.; Pai, M.; Blomme, E. A.; Hsieh, G. C.; Decker, M. W.; Honore, P. Pharmacological modulation of movement-evoked pain in a rat model of osteoarthritis. *Eur. J. Pharmacol.* **2009**, *613*, 39–45.

(35) Ivanavicius, S. P.; Ball, A. D.; Heapy, C. G.; Westwood, F. R.; Murray, F.; Read, S. J. Structural pathology in a rodent model of osteoarthritis is associated with neuropathic pain: increased expression of ATF-3 and pharmacological characterization. *Pain* **2007**, *128*, 272–282.

(36) Pomonis, J. D.; Boulet, J. M.; Gottshall, S. L.; Phillips, S.; Sellers, R.; Bunton, T.; Walker, K. Development and pharmacological characterization of a rat model of osteoarthritis pain. *Pain* **2005**, *114*, 339–346.

(37) Vonsy, J. L.; Ghandehari, J.; Dickenson, A. H. Differential analgesic effects of morphine and gabapentin on behavioural measures of pain and disability in a model of osteoarthritis pain in rats. *Eur. J. Pain* **2008**, *8*, 786–793.

(38) Bendele, A. M. Animal models of osteoarthritis. *J. Musculoskel. Neuron Interact.* **2001**, *1*, 363–376.

(39) Bendele, A. M. Animal Models. In *Bone and Osteoarthritis* Bronner, F.; Farach-Carson, M. C., Eds.; Springer-Verlag: London, 2007; pp 149–163.

(40) Gerwin, N.; Bendele, A. M.; Glasson, S.; Carlson, C. S. The OARSI histopathology initiative - recommendations for histological assessments of osteoarthritis in the rat. *Osteoarthritis Cartilage* **2010**, *18*, S24–S34.

(41) Latourte, A.; Richette, P. Inhibition of ADAMTS-5: the right target for osteoarthritis? *Osteoarthritis Cartilage* **2022**, *30*, 175–177.

(42) Peterson, J. T. The importance of estimating the therapeutic index in the development of matrix metalloproteinase inhibitors. *Cardiovasc. Res.* **2006**, *69*, 677–687.